RBM45 Modulates the Antioxidant Response in Amyotrophic Lateral Sclerosis through Interactions with KEAP1

Nadine Bakkar, Arianna Kousari, Tina Kovalik, Yang Li, Robert Bowser

Divisions of Neurology and Neurobiology, Barrow Neurological Institute, St. Joseph's Hospital and Medical Center, Phoenix, Arizona, USA

Amyotrophic lateral sclerosis (ALS) is a fatal neurodegenerative disease characterized by the selective loss of motor neurons. Various factors contribute to the disease, including RNA binding protein dysregulation and oxidative stress, but their exact role in pathogenic mechanisms remains unclear. We have recently linked another RNA binding protein, RBM45, to ALS via increased levels of protein in the cerebrospinal fluid of ALS patients and its localization to cytoplasmic inclusions in ALS motor neurons. Here we show RBM45 nuclear exit in ALS spinal cord motor neurons compared to controls, a phenotype recapitulated *in vitro* in motor neurons treated with oxidative stressors. We find that RBM45 binds and stabilizes KEAP1, the inhibitor of the antioxidant response transcription factor NRF2. ALS lumbar spinal cord lysates similarly show increased cytoplasmic binding of KEAP1 and RBM45. Binding of RBM45 to KEAP1 impedes the protective antioxidant response, thus contributing to oxidative stress-induced cellular toxicity. Our findings thus describe a novel link between a mislocalized RNA binding protein implicated in ALS (RBM45) and dysregulation of the neuroprotective antioxidant response seen in the disease.

Amyotrophic lateral sclerosis (ALS) is a fatal idiopathic adult-onset neurodegenerative disease characterized by a loss of motor neurons in the brain, brain stem, and spinal cord, with consequent atrophy of associated muscles (1, 2). Incidence rates are 1 to 3 cases per 100,000 individuals per year. Pathogenic mechanisms underlying the disease are not fully understood. Approximately 5 to 10% of all ALS cases are familial (3), with the remaining cases being termed sporadic, contributing to the clinical heterogeneity within the patient population. Nevertheless, typical hallmarks of ALS include neuronal atrophy, mitochondrial dysfunction, excitotoxicity, oxidative stress, and ubiquitinated cellular inclusions (4, 5). A growing number of genes with diverse functions have been implicated in the disease etiology. Mutations in a number of RNA binding proteins have been linked to ALS, including TAR DNA binding protein 43 (TDP-43) and Fused in Sarcoma (FUS) (6). Mutations in these genes result in reduced levels in the nucleus and their accumulation in cytoplasmic ubiquitin-positive inclusions (7). Both TDP-43 and FUS possess prion-like domains and relocate to cytoplasmic stress granules under stress conditions, suggesting potential pathology commonalities (8). Genetic alterations in these and other RNA binding proteins link RNA metabolism to the pathobiology of ALS.

Recently, we linked another RNA binding protein, RBM45, to ALS using a proteomic screen of cerebrospinal fluid (CSF) from ALS and control subjects (9). RBM45, also known as Drb1, was first identified as a novel RNA binding protein that functions in neural development (10). RBM45 possesses three RNA recognition motifs (RRMs) as well as a C-terminal nuclear localization sequence (10). By using a large liquid chromatography-tandem mass spectrometry (LC-MS/MS) unbiased proteomic analysis of CSF from 250 subjects, RBM45 levels were found to be increased in the CSF of ALS patients (9). ALS spinal cord motor neurons exhibited RBM45-positive cytoplasmic inclusions bearing a striking resemblance to those seen with TDP-43 and FUS in ALS motor neurons, and colocalization between TDP-43 and RBM45 in cytoplasmic inclusions was observed (9). Extensive RBM45 pathology was observed in patients with *C9ORF72* repeat expansions. RBM45 was subsequently found to bind and colocalize with

the C-terminal fragment of TDP-43 implicated in ALS (11), consistent with a role for RBM45 in ALS pathobiology.

Neurons are particularly susceptible to degeneration via redox dysregulation, as the high oxygen consumption by the brain results in a significant production of reactive oxygen species (ROS) (12), so it is no surprise that oxidative stress plays a significant role in the pathogenesis of ALS and other neurodegenerative diseases. Evidence for oxidative damage to proteins and lipids has been detected in serum, fibroblasts, and the central nervous system (CNS) of ALS patients as well as various organs in the G93A mutant SOD1 transgenic murine model of ALS (13–20). A central regulator of cellular responses to oxidative stress is the NRF2 (NF-E2-related factor 2)/KEAP1 (Kelch-like ECH-associated protein 1) pathway. NRF2 is a basic-region leucine zipper transcription factor with a transactivation domain in the N terminus and a DNA binding region in the C terminus (21). NRF2 is negatively regulated by the actin-binding cytosolic protein KEAP1. KEAP1 homodimers bind NRF2 through its C terminus, while through its N-terminal end, it associates with Cullin 3 (Cul3) to form an E3 ubiquitin ligase complex, in which KEAP1 serves as a substrate adaptor (22). Under normal basal conditions, NRF2 is constitutively polyubiquitinated by this KEAP1-Cul3 ubiquitin ligase complex, targeting it for proteasomal degradation. When the cell is exposed to oxidative stress conditions, cysteine residues on KEAP1 become oxidized, leading to its dissociation from NRF2 and the subsequent translocation of NRF2 to the nucleus to drive

the expression of antioxidant response genes (23). More recently, endogenous intracellular stress was shown to induce NRF2 activity through p62, a polyubiquitin binding protein that targets substrates for autophagy. When intracellular stress impairs autophagy, p62-containing protein aggregates accumulate as inclusion bodies containing KEAP1, thus releasing NRF2 for nuclear translocation and induction of cytoprotective genes (24). NRF2 drives the expression of >200 genes involved in the cellular antioxidant and anti-inflammatory defense, binding to a regulatory enhancer region called the antioxidant response element (ARE) (25). ARE-containing genes include detoxification enzymes, extracellular superoxide dismutase, heat shock proteins, as well as the pro- and anti-inflammatory cyclooxygenase 2 (COX-2), heme oxygenase 1 (HO-1), and inducible nitric oxide synthase (iNOS).

The NRF2/KEAP1 pathway is altered both in animal models of ALS and in postmortem tissues from ALS patients. Mimoto et al. observed dramatic increases in NRF2 immunoreactivity and total protein levels in motor neurons and lumbar spinal cord of SOD1 mutant transgenic mice, with a concomitant decrease in KEAP1 protein levels, although downstream gene expression was only modestly increased, suggesting an impairment of the NRF2/KEAP1 pathway (26). By crossing ARE reporter mice with G93A mutant SOD1 mice, NRF2 activation was observed in skeletal muscles at postnatal day 60, prior to phenotypic disease onset, with subsequent later activation in spinal cord motor neurons (27). Knockout of *Nrf2* in G93A mutant SOD1 mice accelerated motor neuron loss and astrocytic proliferation (28). Selective overexpression of *Nrf2* in neurons or type II skeletal muscle fibers delayed disease onset but failed to extend the survival of G93A mutant SOD1 mice (29), while its overexpression in astrocytes had beneficial effects on survival and decreased glial activation (30), thus highlighting the complexity of this pathway in the various cell types involved in ALS.

ALS postmortem brain and spinal cord exhibited reduced NRF2 RNA and protein levels, while KEAP1 mRNA but not protein levels increased, thus highlighting the deregulated antioxidant response pathway in ALS (31). More recently, KEAP1 was observed in p62-containing neuronal cytoplasmic inclusions in various neurodegenerative diseases, including ALS (32). However, localization with other proteins that form cytoplasmic inclusions during ALS was not investigated. Mutant TDP-43 has been shown to induce oxidative stress and subsequent nuclear accumulation of NRF2 in cell culture, while motor cortexes from TDP-43 A315T transgenic mice show significant increases in the levels of the NRF2 target HO-1 (33, 34). These data indicated that there is a deregulation of the linear KEAP1/NRF2/ARE pathway in ALS, a deregulation associated with the sequestering of KEAP1 in ubiquitinated pathological inclusions and poor induction of cytoprotective ARE gene products.

In this study, we have uncovered a role for RBM45 in modulating cellular responses to oxidative stress. We show that oxidative insults result in a redistribution of RBM45 from the nucleus to the cytoplasm, accompanied by stress granule formation reminiscent of the phenotype in ALS patients described previously. In addition, we demonstrate that RBM45 binds to and regulates KEAP1 levels in various cell lines as well as the ALS spinal cord. This RBM45/KEAP1 interaction impedes the antioxidant response and contributes to increased cell death. Our findings thus provide a novel mechanistic link between deregulated ALS inclu-

TABLE 1 Primers used for real-time PCR analysis

Primer	Sequence
p62-For	AGC TGC CTT GTA CCC ACA TC
p62-Rev	CAG AGA AGC CCA TGG ACA G
HO1-For	CCA GCA ACA AAG TGC AAG ATT C
HO1-Rev	TCA CAT GGC ATA AAG CCC TAC AG
NQO1- For	GTC ATT CTC TGG CCA ATT CAG AGT
NQO1-Rev	TTC AGG ATT TGA ATT CGG G
GAPDH-For	GAA ATC CCA TCA CCA TCT TCC AGG
GAPDH-Rev	GAG CCC CAG CCT TCT CCA TG
Cyclophilin-For	CCCCACCGTGTTCTTCGACA
Cyclophilin-Rev	CCCAGTGCTCAGAGCACGAAA
ratRBM45-For	GCTATCTCCAAACGCCTGTC
ratRBM45-Rev	GGGACGATGTCAAAAATGCT
hNQO1-ARE-For	CCCTTTTAGCCTTGGCACGAAA
hNQO1-ARE-Rev	TGCACCCAGGGAAGTGTGTTGTAT

sion-forming RBM45 and the NRF2/KEAP1 oxidant stress response.

MATERIALS AND METHODS

Antibodies and materials. Antibodies against KEAP1 (catalog numbers 60027 and 10503), TDP-43 (catalog number 60019), and FUS were obtained from Proteintech, and antibody to hemagglutinin (HA) (clone 3F10) was obtained from Roche. NRF2 antibodies were purchased from Abcam (catalog number 31163) and Novus Biologicals (catalog number H00004780), while glyceraldehyde-3-phosphate dehydrogenase (GAPDH) was obtained from Cell Signaling Technology. p62 (anti-sqstm1) and HO-1 (heme oxygenase) antibodies were obtained from Novus Biologicals (catalog numbers H00008878-M01 and NBP1-31341, respectively), and TIAR was obtained from BD (catalog number 610352). RBM45 antibodies were obtained from Sigma-Aldrich (catalog number HPA020448) or custom-made against the C terminus or the middle of human RBM45 (Pacific Immunology). Anti-Flag M2 affinity gel, mouse IgG-agarose beads, and the monoclonal anti-Flag antibody (clone M2) were obtained from Sigma-Aldrich. Hydrogen peroxide (H$_2$O$_2$), *tert*-butyl hydroquinone (tBHQ), and Paraquat (methyl viologen dichloride hydrate) were purchased from Sigma-Aldrich and used fresh. Pierce protein A/G-agarose beads were obtained from Thermo Scientific. Secondary antibodies for immunofluorescence were obtained from Invitrogen, and antibodies used for Western blot analysis were obtained from LiCor.

Plasmids. The RBM45 expression plasmid was purchased from the DNAsu plasmid repository at the Arizona State University Biodesign Institute and cloned into a pcDNA3 vector. QuikChange XL mutagenesis (Stratagene) was used to delete the RBM45 nuclear localization signal (NLS), and truncation mutants were cloned from the wild-type RBM45 backbone by PCR. The pGL3-ARE-luciferase construct was kindly provided by D. Zhang (University of Arizona, Tucson, AZ). pcDNA3-HA2-KEAP1 (Addgene plasmid 21556) and pcDNA3-My3-NRF2 (Addgene plasmid 21555) expression plasmids were obtained from Y. Xiong (University of North Carolina at Chapel Hill) (35). KEAP1 truncation mutants were generated from the full-length KEAP1 plasmid, in a pcDNA3 backbone.

Gene expression analysis. For quantitative RNA expression, total RNAs from multiple neuronal preparations were prepared by using the Quick-RNA miniprep kit from Zymo Research. cDNA was synthesized, and real-time reverse transcription-PCR (RT-PCR) was performed by using FastStart Universal Sybr green master mix (Roche). Amplification values were normalized to cyclophilin housekeeping gene values, and averages across multiple experiments were computed. Primers used are listed in Table 1.

Tissue samples. ALS and nonneurologic disease control postmortem tissue samples were obtained from the University of Pittsburgh ALS Tis-

TABLE 2 Subject demographics and RBM45 inclusions in motor neurons[a]

Case	Group	Age (yr)	Gender	PMT (h)	Presence of RBM45 inclusions in motor neurons
CON1	Control	53	F	4	No
CON2	Control	95	M	20	No
CON3	Control	76	M	13	No
CON4	Control	51	F	5	No
ALS1	ALS	48	F	5	Yes
ALS2	ALS	63	F	4	Yes
ALS3	ALS	50	F	7	No
ALS4	ALS	60	F	2	ND
ALS5	ALS	40	M	6	Yes
ALS6	ALS	43	M	6	Yes
ALS7	ALS	73	F	11	ND
ALS8	ALS	69	M	5	No
ALS9	ALS	60	F	4	Yes
ALS10	ALS	68	M	4	Yes

[a] M, male; F, female; PMT, postmortem time; ND, not determined.

sue Bank. All tissue samples were collected after informed consent was obtained from the subjects' next of kin. The consent process was approved by the University of Pittsburgh Institutional Review Board/University of Pittsburgh Committee for Oversight of Research Involving the Dead. Clinical diagnoses were made by board-certified neuropathologists according to consensus criteria for ALS. Subject demographics are listed in Table 2, as is the presence or absence of RBM45 inclusions in motor neurons, as determined in our previous study (9). Statistical analysis was performed by using the Student t test.

Immunoprecipitation and immunoblot analysis. Whole-cell lysates were prepared in radioimmunoprecipitation assay (RIPA) buffer supplemented with protease and phosphatase inhibitors (Sigma and Roche, respectively). For immunoprecipitation (IP), cells were fractionated by using a low-detergent buffer (10 mM HEPES [pH 7.6], 60 mM KCl, 1 mM EDTA, and 0.25% NP-40) and spun at 600 × g for 5 min to separate the cytoplasmic protein fraction from nuclei. Immunoprecipitations were performed on proteins from the cytoplasmic fraction (200 to 300 μg) by first preclearing the lysates with isotype-specific IgG and then incubating them with a pre-cross-linked antibody-agarose complex overnight. Samples were then washed with RIPA buffer for 20 to 30 min at 4°C, before boiling in SDS loading dye, spinning, and loading onto gels for Western blot analysis. Gels were transferred onto Immobilon FL polyvinylidene difluoride (PVDF) membranes (Millipore), blocked in Odyssey blocking buffer, and probed with primary and secondary antibodies (1:15,000 dilution; LiCor). Signals were imaged by using the Odyssey CLx imager (LiCor). All assays were performed in triplicate unless indicated otherwise. For RNase treatment, cytoplasmic protein fractions were incubated with RNase A (catalog number R4642; Sigma) immediately following lysis and prior to preclearing and incubation with antibodies. Immunoprecipitation and washes were then performed as described above.

Lumbar spinal cord tissue homogenates were prepared from frozen tissue from controls (n = 4) and ALS cases (n = 9) for Western blot analysis and coimmunoprecipitation studies. The age ranges and postmortem intervals for this patient subgroup did not statistically differ from those of all subjects or across subgroups (Table 2). Nuclear and postnuclear extracts were prepared as described previously (36). Briefly, samples were homogenized in a solution containing 10 mM Tris (pH 8.0), 10 mM MgCl$_2$, 15 mM NaCl, and 0.5 mM phenylmethylsulfonyl fluoride (PMSF) supplemented with protease and phosphatase inhibitors, and nuclei were collected via low-speed centrifugation at 800 × g for 5 min. The resulting supernatant was saved as the postnuclear extract and used for Western blotting or immunoprecipitation (50 to 70 μg protein per

sample). Densitometric analysis was performed by using ImageStudio 4.0 software from LiCor.

Chromatin immunoprecipitation. Chromatin immunoprecipitation (ChIP) analysis was performed according to a protocol provided by Upstate Biotechnology, Inc. Briefly, cells were cross-linked in 1% formaldehyde, centrifuged, and resuspended in a solution containing 2% SDS, 10 mM EDTA, 50 mM Tris-HCl, and protease inhibitors. Following sonication, one-third of the lysate was precipitated overnight by using a rabbit monoclonal NRF2 antibody (AB 62352/EP1808Y; Abcam) or rabbit IgG. Salmon sperm DNA-protein A-agarose beads (catalog number 16-157; Millipore) were subsequently added, and the mixture was incubated for 5 h at 4°C. Following washes in low-salt buffer (0.1% SDS, 1% Triton X-100, 2 mM EDTA, 20 mM Tris-HCl [pH 8], and 150 mM NaCl), high-salt buffer (0.1% SDS, 1% Triton X-100, 2 mM EDTA, 20 mM Tris-HCl [pH 8], and 500 mM NaCl), and LiCl buffer (0.25 mM LiCl, 1% NP-40, 1% deoxycholate, 1 mM EDTA, and 10 mM Tris-HCl [pH 8.0]), the DNA complex was eluted in 1% SDS–0.1 mM NaHCO$_3$. The eluant was subsequently heated to 65°C for 14 h to reverse cross-link the complexes, and DNA was precipitated. DNA was then purified by using the QIAquick PCR purification kit (Qiagen), and PCRs were performed to amplify a region in the ARE of the NADPH quinone oxidoreductase 1 (NQO1) promoter (25). Primers are listed in Table 1. Samples were run in triplicates, and values were normalized to individual inputs. Enrichment was calculated as fold increase over the IgG control IP.

Cell culture, transfections, and luciferase assay. Neuro2a (murine) and SH-SY5Y (human) neuroblastoma cell lines were purchased from the ATCC and cultured as recommended by the supplier. Both cell lines were differentiated on laminin-coated plates in the presence of 10 μM retinoic acid. NSC-34, Neuro2a, and HEK-293 cells were cultured in Dulbecco's modified Eagle's medium (DMEM) supplemented with 10% fetal bovine serum (FBS). Primary motor neurons were isolated from the spinal cords of Sasco Sprague-Dawley rat embryos at gestation day 14 (E14), as previously described (36). Cells were maintained on poly-D-lysine/human placental laminin-coated plates, in neurobasal medium supplemented with a mix of growth factors, and half of the medium was changed every other day (37). The resulting cultures contained 93 to 98% neurons, as determined by HB9 staining. Cultures were used at days 5 to 6 postisolation for immunofluorescence or protein/RNA isolation. Results from cell lines were confirmed in 4 or 5 independent experiments.

Small interfering RNA (siRNA) for RBM45 was obtained from Dharmacon, Inc., and transfections were performed by using Lipofectamine 2000 (Invitrogen). HEK-293 and Neuro2a cells were cultured in 24-well plates and transfected with 0.15 μg total DNA per well for luciferase assays. Cells were lysed 24 to 48 h later in mammalian protein extraction reagent (M-PER; Pierce) and processed for firefly luciferase and β-galactosidase (β-Gal) assays. Triplicate wells were used for each experiment, and the results shown are from a representative experiment performed in triplicate.

Viability and cellular stress assays. Viability assays were performed by using the CellTox green cytotoxicity assay from Promega (catalog number G8741), according to the manufacturer's recommendations, using a 1:500 dilution of the CellTox green dye in assay buffer (endpoint detection method). Five wells per group were used for each experiment, and the experiments were repeated 3 times. Data from a representative experiment are shown.

Measurement of ROS was performed by using the 2′,7′-dichlorofluorescin diacetate (DCFDA) cellular reactive oxygen species detection assay kit from Abcam, according to the manufacturer's recommendations. Briefly, triplicate cells were incubated with 25 μM DCFDA fluorogenic dye for 45 min at 37°C before phosphate-buffered saline (PBS) washes. Cells were then treated in the supplied buffer supplemented with serum, and fluorescence was read at the indicated time points. Representative data from 2 experiments are shown.

An assay of glutathione content was performed on cells by using the luminescence-based GSH/GSSG-Glo assay from Promega, as suggested

by the manufacturer. This kit allows the measurement of both oxidized and total glutathione levels in order to compute the ratios of reduced to oxidized glutathione. Briefly, the cells are lysed in total glutathione or oxidized glutathione lysis buffer directly in the culture wells following treatments, followed by the addition of luciferin. Luminescence is then read, and background readouts are subtracted from all measurements. Five wells per experimental group were used.

Immunofluorescence. For immunofluorescence assays, cells were plated onto coverslips, treated for different time points, and then fixed with ice-cold methanol for 10 min. The cells were then blocked by using the Scytek Super Block reagent (catalog number AAA125) for 45 min, treated with appropriate primary and secondary antibodies (Alexa Fluor 488 or 594) for 1 h each, washed extensively in PBS, and mounted in aqueous mounting medium (Gelvatol) for imaging. Nuclei were labeled with 4′,6-diamidino-2-phenylindole (DAPI) nuclear stain (1:5,000; Invitrogen). Slides were imaged on a Zeiss AxioVision microscope. Images were deconvolved by using Hyugens Essential software (38). To calculate the percentage of cells with stress granules, we defined granules as cytoplasmic puncta larger than 100 nm and counted the number of cells with RBM45-positive granules. Percentages of granules per cell were calculated as $100 \times$ [(number of cells with granules)/(total number of nuclei)]. At least 100 cells were examined per group, and data presented are the results from three independent experimental sets.

RESULTS

RBM45 is regulated by oxidative stress *in vitro* and in ALS spinal cord. We previously demonstrated that RBM45 was contained in cytoplasmic inclusions of neurons within the brain and spinal cord of ALS patients (9). Although the levels of RBM45 were increased in the CSF of ALS patients, little is known about its function. We sought here to characterize the function of this protein and identify conditions that induce its accumulation in the cytoplasm to better understand its role in ALS. The RBM45 protein localizes predominantly to the nucleus in various neuronal and nonneuronal cell lines, although a small portion of the protein is found in the cytoplasm and neuronal processes (data not shown). We postulated that cellular stress may regulate RBM45 subcellular distribution, as both TDP-43 and FUS translocate into cytoplasmic granules in response to stress. To test this hypothesis, we treated primary rat motor neurons with various stressors and examined RBM45 subcellular distribution. We chose doses of two stressors, H_2O_2 and Paraquat, that induced no more than 30 to 40% cell death over 24 h in an attempt to mimic chronic stress and then monitored RBM45 subcellular distribution. We observed that RBM45 redistributed to the cytoplasm in response to either H_2O_2 or Paraquat, as detected by using an RBM45-specific antibody (Fig. 1A). Cytoplasmic granules containing RBM45 were most evident in Paraquat-treated cells (Fig. 1A), and increasing levels of this stressor generated an increasing number of cells with RBM45 granules. These results were verified by using a second RBM45 antibody directed against a different epitope of the protein (data not shown). Paraquat is a potent reactive oxygen species producer that interferes with the electron transfer system and was previously shown to alter the subcellular localization of another ALS-linked RNA binding protein, TDP-43, to cytoplasmic stress granules (39). Similar results were seen in Paraquat-treated differentiated SH-SY5Y but not HEK-293 or undifferentiated NSC-34 cells. No significant differences in the protein or RNA levels of RBM45 were seen with either cell stressor (Fig. 1B and data not shown).

Given the nuclear exit of RBM45 in response to oxidative stress, we asked whether we could see such an effect on ALS patient tissues. Cytoplasmic extracts from lumbar spinal cord tissue

homogenates were examined by RBM45 Western blotting. The results showed a significant increase in RBM45 levels in the soluble cytoplasmic fraction in ALS patient spinal cords compared to nonneurologic controls (Fig. 1C). No significant changes in total RBM45 levels (Fig. 1D) were observed, consistent with our previously reported findings (9). Given that oxidative stress is a well-reported pathogenic factor in ALS, these results support that RBM45 subcellular distribution is regulated by oxidative stress both *in vitro* and *in vivo*.

To characterize RBM45-containing cytoplasmic granules generated under stress conditions, we performed double-label immunofluorescence microscopy using markers of cytoplasmic stress granules. We first examined RBM45 colocalization with the stress granule marker TIAR. TIAR is an RNA binding protein that binds and accumulates untranslated mRNA under conditions of stress, including Paraquat treatment (40). When primary motor neurons were treated with Paraquat, TIAR relocalized from the nucleus to cytoplasmic stress granules (Fig. 2A), as previously reported (41). Interestingly, RBM45 colocalized with TIAR in granules, indicating that RBM45 was a constituent of Paraquat-induced cytoplasmic stress granules (Fig. 2A).

Next, we asked whether RBM45 colocalizes with the p62/sequestosome protein in response to oxidative stress. p62, a polyubiquitin binding protein, recognizes polyubiquitinated protein aggregates and targets them for autophagic degradation (42). Various mutations in *p62* have been identified in ALS, and the protein has been shown to localize to cytoplasmic inclusions in motor neurons (43–46). When primary motor neurons were treated with Paraquat, p62 formed round cytoplasmic inclusions that colocalized with RBM45 (Fig. 2B), consistent with the ubiquitin-positive RBM45 cytoplasmic inclusions observed in ALS spinal cord motor neurons (9).

Since oxidative stress activates the antioxidant response pathway by targeting the NRF2 inhibitor KEAP1 for proteasomal degradation, and given that KEAP1 has been shown to localize to p62-positive neuronal cytoplasmic inclusions in neurodegenerative diseases (32), we tested the hypothesis that KEAP1 and RBM45 colocalize in response to Paraquat. KEAP1 displays a diffuse cytoplasmic immunostaining pattern in untreated primary motor neurons, with little overlap with RBM45 that is located predominantly in the nucleus (Fig. 2C). Upon Paraquat treatment, KEAP1 is redistributed into cytoplasmic granules that often contain RBM45 (Fig. 2C, arrowheads).

RBM45 binds the antioxidant response member KEAP1. To further define the role of RBM45 in the antioxidant response and its interaction with KEAP1, we performed coimmunoprecipitation studies. A previously reported unbiased proteomic study to discover KEAP1-interacting proteins identified RBM45 as a high-confidence interacting protein (47). To validate these findings as well as our *in vitro* data, we used HEK-293 cells and two available RBM45 antibodies to immunoprecipitate RBM45 and determine if KEAP1 was detected among the coprecipitated proteins. Indeed, and by using both RBM45 antibodies but not an isotype IgG control, we detected KEAP1 interactions with RBM45 (Fig. 3A, left). This interaction was validated by using a reverse IP, using anti-KEAP1 antibody to pull down RBM45 (Fig. 3A, right). RBM45/ KEAP1 interactions were also observed in overexpression cell culture systems where RBM45 or both the RBM45 and KEAP1 proteins were transfected (data not shown). To assess the physiological relevance of such interactions, we repeated these binding studies with two neuroblastoma cell lines (SH-SY5Y and
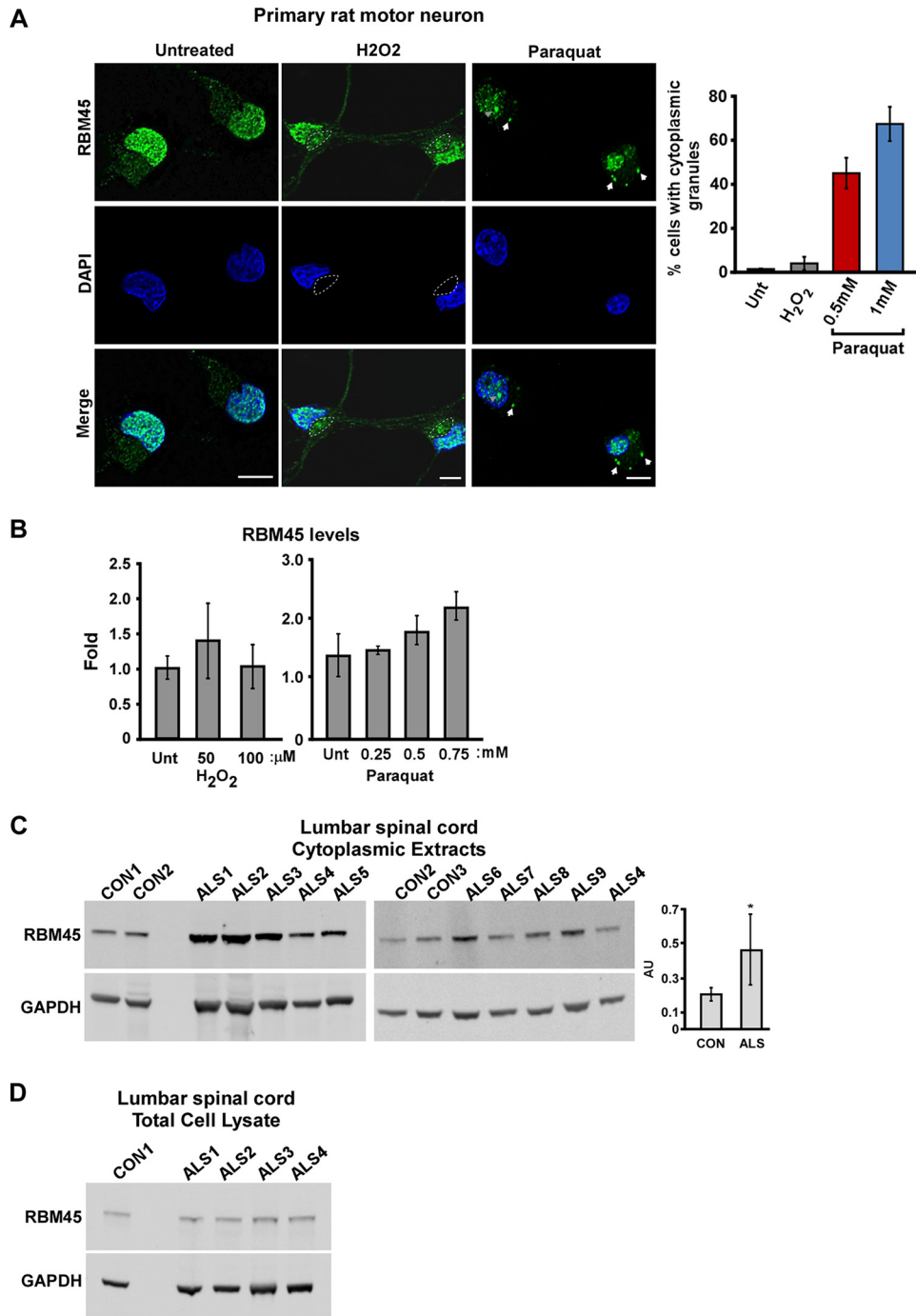
FIG 1 (A) Primary rat motor neurons were cultured for 5 days and then treated with 200 μM H_2O_2 or 1 mM Paraquat for 16 h. Cells were fixed in methanol and stained with RBM45 (C-terminal antibody). Nuclei were costained with DAPI. The outlined area (middle) highlights the cytoplasmic compartment. Cytoplasmic granules are denoted by arrows, while nuclear granules are indicated by arrowheads. Bars, 10 μm. The graph shows the quantification of the number of cells with granules in primary motor neurons treated with 200 μM H_2O_2 or 0.5 or 1 mM Paraquat for 16 h. At least 100 cells were assayed per group per experiment, and the results shown are averages from 3 different experiments. (B) Rat motor neurons were prepared from 5 separate cultures and treated with different doses of H_2O_2 or Paraquat for 16 h. RNA was then prepared, and real-time PCR for RBM45 was performed. Results were normalized to cyclophilin mRNA values, and the graphs represent average data from the 5 independent replicates. (C) Cytoplasmic fractions from lumbar spinal cords of ALS or control subjects were analyzed by Western blotting. Membranes were probed for RBM45 or GAPDH. The graph represents data from densitometric analyses of RBM45 normalized to GAPDH for individual samples, and averages are plotted (the asterisk denotes a P value of <0.05). AU, arbitrary units. (D) Twenty micrograms of whole-cell lumbar spinal cord homogenates from one control and four ALS patients was run on a Western blot and probed for RBM45 or GAPDH.
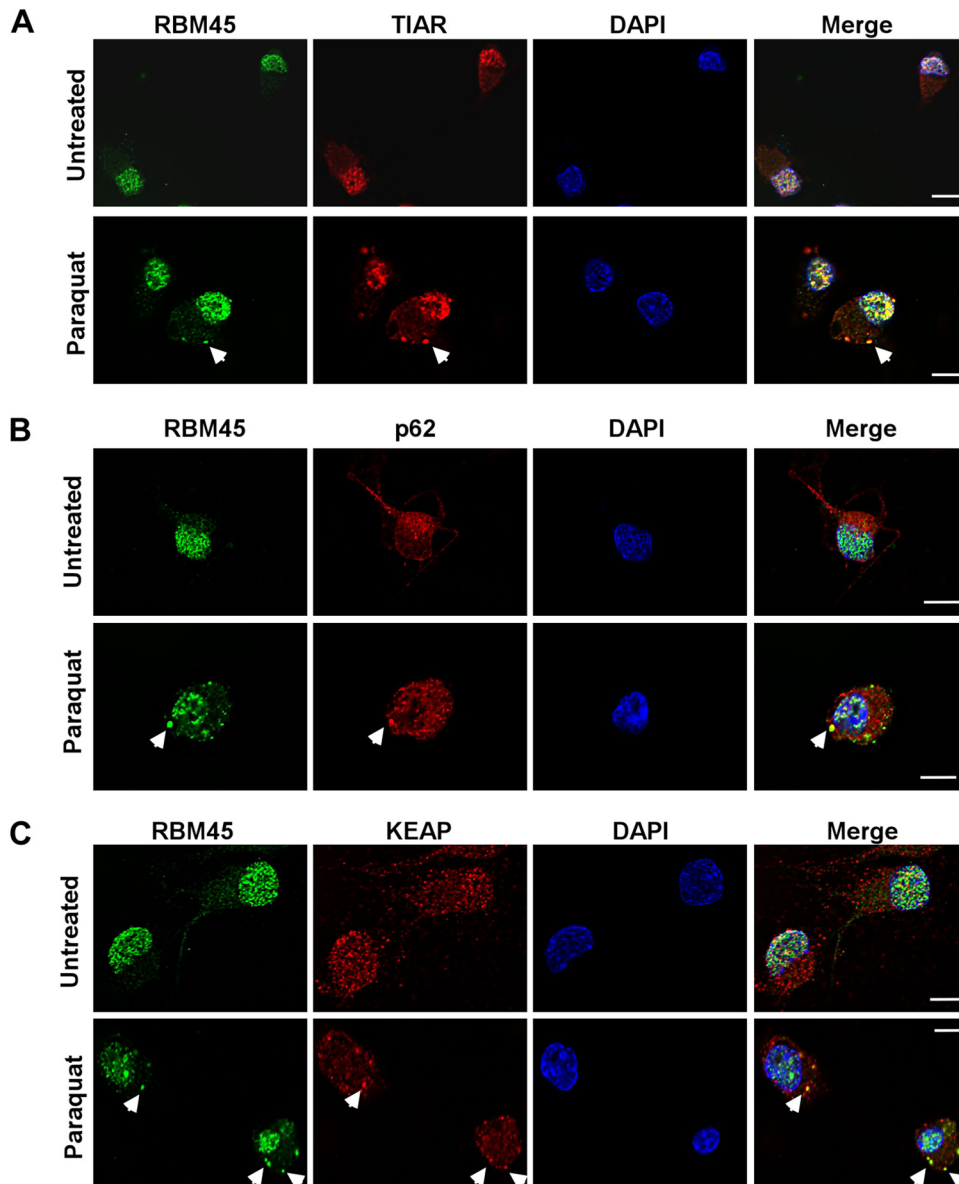
FIG 2 Primary rat motor neurons were cultured for 5 days and treated with 1 mM Paraquat for 16 h. Cells were fixed with methanol and double stained for RBM45 (C-terminal antibody in green) and either TIAR (A), KEAP1 (B), or p62 (C) (in red). Nuclei are stained with DAPI. Arrowheads indicate the colocalization of the two proteins in stress granules. Bars, 10 μm.

Neuro2a) (data not shown) as well as human lumbar spinal cord tissue (Fig. 3B). Again, KEAP1 was identified as interacting with RBM45, confirming our findings that RBM45 is a novel KEAP1 binding partner.

Next, we mapped the amino acid domains of RBM45 mediating binding to KEAP1. We generated different truncation deletions of RBM45 as well as an NLS deletion construct (RBM45-ΔNLS) that localizes solely to the cytoplasm (Fig. 3C). These constructs were each transfected into a HA-KEAP1-overexpressing HEK-293 stable cell line, and coimmunoprecipitations were performed by using cytoplasmic fractions. Not surprisingly, wild-type RBM45 overexpression resulted in increased binding to KEAP1 compared to the vector control (Fig. 3C). When RBM45 expression was restricted to the cytoplasm by using the RBM45-

ΔNLS or RBM45-(1–195) truncation mutant, an increased interaction with KEAP1 was observed, due to the increased pool of RBM45 available in the cytoplasm for binding. Interestingly, the highest level of binding between RBM45 and KEAP1 was observed with an RBM45 truncation expressing the first two RNA binding domains, RBM45-(1–195). RBM45 amino acids 196 to 474 failed to bind KEAP1, demonstrating a specific interaction between KEAP1 and RBM45 N-terminal amino acids 1 to 195, which are necessary and sufficient for binding to KEAP1. This interaction, although mediated by the RNA binding domains of RBM45, was not RNA dependent, as RNase A treatment had no effect on this interaction (Fig. 3D).

To determine the region of KEAP1 required for binding to RBM45, we generated KEAP1 truncations and expressed each
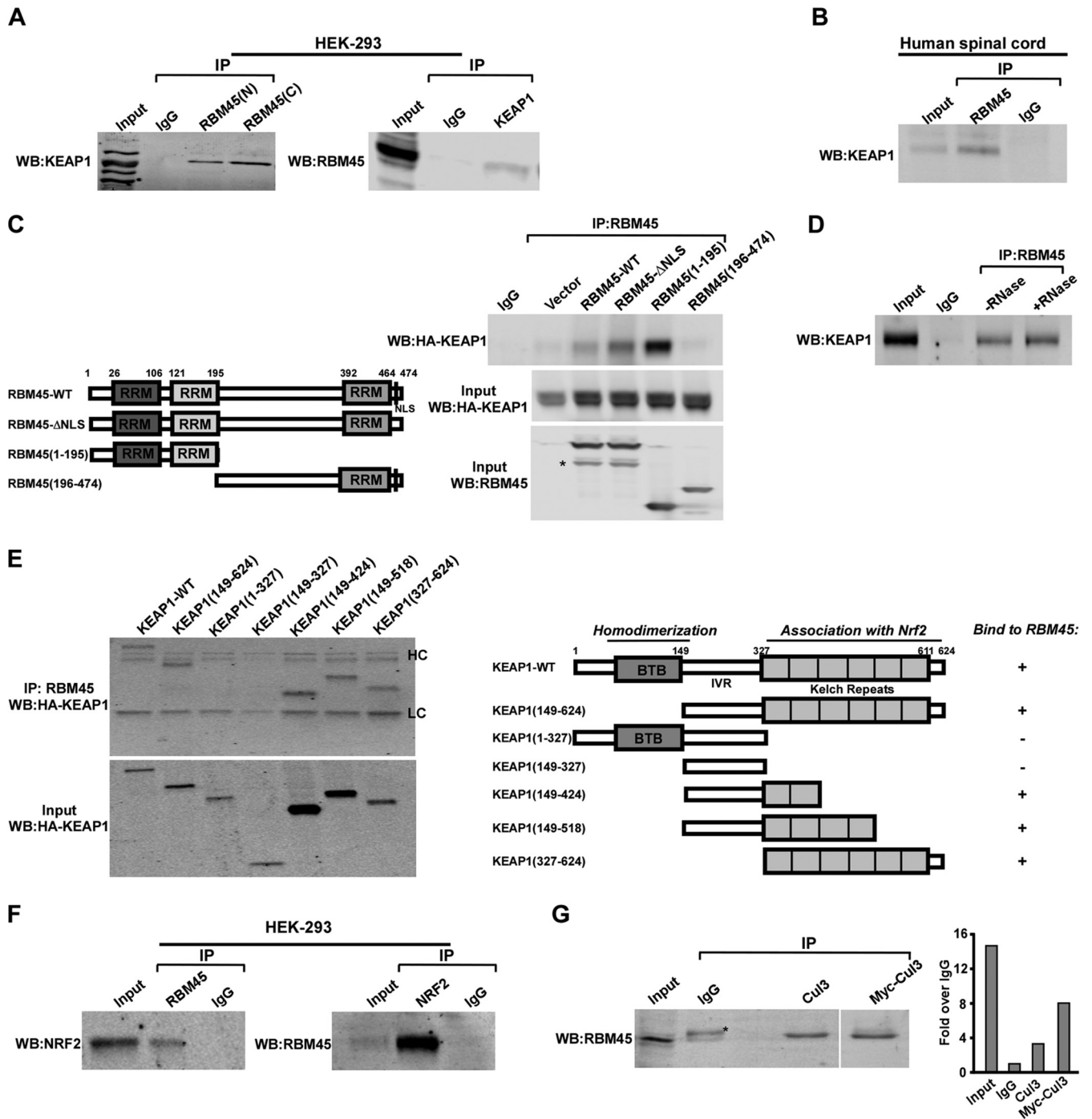
FIG 3 (A) HEK-293 cells were lysed in low-detergent buffer, and the cytoplasmic fractions were used for coimmunoprecipitation of RBM45 (left), KEAP1 (right), or an isotype-specific control IgG antibody. The input is a dilution of the starting cytoplasmic lysate used for immunoprecipitation (IP). Membranes were probed for KEAP1 (left) or RBM45 (right). (B) Cytoplasmic lumbar spinal cord lysates from a control patient were incubated with RBM45 antibody or an IgG control, and immunoprecipitation was performed as described above for panel A. Membranes were probed for KEAP1. (C) The HEK-293 cell line expressing HA-KEAP was transfected with the empty vector control, wild-type RBM45, an RBM45 mutant lacking the nuclear localization signal (RBM45-ΔNLS), or various RBM45 truncations. Cells were lysed, and RBM45 was immunoprecipitated from cytoplasmic fractions. Eluates were analyzed by Western blotting (WB) and probed for HA-KEAP. The asterisk indicates a nonspecific band detected in two input lanes. (D) HEK-293 cells expressing RBM45 were lysed, and cytoplasmic fractions were incubated with RNase A prior to immunoprecipitation, as described above for panel C. Western blotting for HA-KEAP was performed. (E) HEK-293 cells expressing wild-type RBM45 were transfected with various KEAP truncation mutants. Cytoplasmic fractions were prepared, and RBM45-bound complexes were immunoprecipitated as described above for panel C. (Top) Eluates were analyzed by Western blotting and probed for HA-KEAP. (Bottom) HA-KEAP Western blot of input material showing the location of each HA-KEAP band within the gel. The schematic at the right shows the various KEAP constructs used in our analysis. IVR, intervening region; BTB, broad-complex Tramtrack and Bric-a-Brac domain; LC, IgG light chain; HC, IgG heavy chain. Shown is a representative blot chosen out of 3 independent experiments. (F) HEK-293 cytoplasmic lysates were prepared, and RBM45 (left) or NRF2 (right) along with isotype IgG controls were immunoprecipitated as described above for panel A. Eluates were analyzed by Western blotting and probed for NRF2 (left) or RBM45 (right). (G) HEK-293 cells were transfected with Myc-Cul3 expression vectors, and antibodies against IgG, Cul3, or the Myc tag were used to immunoprecipitate Cul3-bound complexes from cytoplasmic fractions, as described above for panel A. Membranes were probed for RBM45. Densitometric analysis was performed on the RBM45 band, and values were plotted as fold increases over the IgG control lane bands.

construct in RBM45-expressing stable cell lines. KEAP1 possesses six C-terminal Kelch repeats necessary for its interaction with NRF2, while its N-terminal end harbors the BTB (broad-complex Tramtrack and Bric-a-Brac) domain that allows homodimerization as well as binding to the Cul3 E3 ligase (21, 22). Our results demonstrate that binding between KEAP1 and RBM45 occurs in the first two Kelch domains of KEAP1, amino acids 327 to 424, as KEAP1(149–424) shows strong binding to RBM45, while the KEAP1(149–327) form does not bind RBM45 (Fig. 3E).

Given that KEAP1 functions in the cytoplasm as part of the KEAP1/NRF2/Cul3 complex, where it binds NRF2 and recruits the ubiquitin ligase machinery, we asked whether the RBM45/KEAP1 interaction occurs within this larger protein complex. To this end, we asked if NRF2 could bind RBM45. While NRF2 levels are kept low in unstimulated cells, we detected NRF2 within proteins coprecipitated with RBM45 (Fig. 3F). Reverse-IP experiments using an NRF2 antibody to pull down RBM45 further confirmed these findings. Similar coimmunoprecipitation experiments showed that RBM45 binds endogenous as well as overexpressed Cul3, although this interaction was weak (Fig. 3G), suggesting that the binding of RBM45 to Cul3 was indirect and possibly occurred via KEAP1. Taken together, these results demonstrate that RBM45 binds KEAP1 within the KEAP1/NRF2/Cul3 antioxidant response pathway.

RBM45/KEAP1 interactions in ALS spinal cord. Having established that RBM45 is a member of the KEAP1/NRF2 antioxidant response complex in cultured cells, we next sought to determine if this interaction occurs *in vivo* in a neurodegenerative disease, such as ALS, that exhibits increased oxidative stress. The KEAP1 RNA level was previously shown to be increased in the motor cortex but not the spinal cord of ALS patients compared to controls, although no significant differences were seen at the protein level (31). We detected increased KEAP1 protein levels in some but not all ALS patient lumbar spinal cord cytosolic fractions compared to controls, but this did not reach statistical significance (Fig. 4A). Nevertheless, since we observed increased cytoplasmic RBM45 levels in ALS, and since we have shown *in vitro* that sequestering of RBM45 in the cytoplasm increases its interaction with KEAP1, we asked whether the RBM45 interaction with KEAP1 changed in ALS. Indeed, we detected a significant increase in KEAP1-RBM45 binding in cytosolic fractions from ALS lumbar spinal cord compared to controls (Fig. 4B). These data are consistent with our *in vitro* findings that cytoplasmic RBM45 binds KEAP1. In addition, given the colocalization of RBM45 and p62 in the cytoplasm of stressed primary rat motor neurons (Fig. 2B), we asked whether RBM45 also binds p62 in ALS patient cytoplasmic extracts. Our results indicate that RBM45 can bind p62 and that RBM45-p62 binding was increased in ALS spinal cords (Fig. 4C). To confirm these findings, we also detected coimmunoprecipitation of p62 and RBM45 from HEK-293 cell cytoplasmic fractions, thus showing that p62 is a cytoplasmic binding partner for RBM45 (Fig. 4D). In addition, overexpression of the RBM45-ΔNLS construct, which enhances cytoplasmic RBM45 levels, increased the pulldown of p62 compared to the wild type (Fig. 4E). Taken together, these data indicated that RBM45 cytoplasmic redistribution that occurs in ALS spinal cord results in increased binding of RBM45 to both KEAP1 and p62.

Cytoplasmic RBM45 increases KEAP1 levels, inhibiting both the basal and activated KEAP1/NRF2/ARE pathways. We next examined the effects of RBM45 on the functional activity of the KEAP1/NRF2/ARE pathway. First, we observed that increasing cytoplasmic RBM45 levels resulted in increased KEAP1 protein levels, while RBM45 knockdown using siRNA oligonucleotides reduced KEAP1 levels (Fig. 5A). KEAP1 mRNA levels were not altered in these experiments, suggesting that RBM45 modulated KEAP1 protein levels. Next, we examined NRF2 levels to determine if they are RBM45 dependent. Wild-type RBM45 (RBM45-WT) and RBM45-ΔNLS decreased NRF2 protein levels, consistent with the regulation of the NRF2 inhibitor KEAP1 (Fig. 5B). Similarly, RBM45-(1–195), which can bind KEAP1, decreased NRF2 protein levels. Conversely, the RBM45-(196–474) mutant, which is unable to bind KEAP1, failed to alter NRF2 protein levels (Fig. 5B), thus indicating that RBM45 regulation of NRF2 occurs via an interaction with KEAP1. Since KEAP1 is a negative regulator of NRF2 activity, we used an ARE-luciferase reporter assay to determine whether RBM45 stabilization of KEAP1 affects downstream NRF2 function. When the reporter was transfected in RBM45-overexpressing cells, decreased NRF2 promoter binding activity was observed compared to control vector-expressing cells. Inhibition of NRF2 function was even more evident when RBM45-ΔNLS was used, consistent with the increased cytoplasmic binding of RBM45 to KEAP1 (Fig. 5C), whereas RBM45 knockdown was associated with enhanced NRF2 activity, consistent with decreased levels of the KEAP1 inhibitor. To corroborate findings on NRF2 DNA binding activity in the presence of decreased RBM45 levels, we performed chromatin immunoprecipitations (ChIPs) on the endogenous NRF2 target gene NADPH quinone oxidoreductase 1 (NQO1) (Fig. 5D). Consistent with the increased ARE binding on the artificial ARE-luciferase promoter, RBM45 knockdown increased the binding of NRF2 on AREs in its target gene NQO1. An NRF2 activator, *tert*-butyl hydroquinone (tBHQ), was used as a positive control to show that the assay can detect changes in NRF2 promoter binding activity (Fig. 5D).

Since reporter and ChIP assays measure only promoter binding activity and not the expression levels of endogenous target genes, we examined the levels of the antioxidant response NRF2 target genes heme oxygenase 1 (HO-1), NQO1, and p62 in cells with RBM45 overexpression. Both wild-type RBM45 and the cytoplasmically sequestered variant (RBM45-ΔNLS) decreased the transcription of the NRF2 target genes HO-1 and NQO1 but not that of p62 (Fig. 5E). HO-1 protein levels were similarly decreased as more RBM45 was overexpressed, reinforcing the negative regulation of RBM45 on this NRF2 target gene (Fig. 5F). Consistent with the decreased levels of antioxidant genes in the presence of increased RBM45 levels, basal levels of reactive oxygen species (ROS) were elevated (Fig. 5G), and the ratio of reduced to oxidized glutathione was decreased, indicating higher levels of oxidized glutathione (Fig. 5H). Taken together, these results demonstrate an increased state of basal oxidative stress in response to increased cytoplasmic levels of RBM45, potentially arising from the inhibited antioxidant pathway.

Given that increased oxidative stress is toxic to cells, we next investigated the effect of increasing levels of cytoplasmic RBM45 on cell viability. While wild-type RBM45 overexpression resulted in a 35% increase in cell death compared to vector control cells, expression of RBM45-ΔNLS or the RBM45-(1–195) truncation, which binds and stabilizes KEAP1, induced a 50% increase in cell death (Fig. 5I), suggesting that this effect is mediated by KEAP1/RBM45 binding. Deletion of the KEAP1 interaction domain of RBM45 [RBM45-(196–474)] greatly reduced cell death to levels
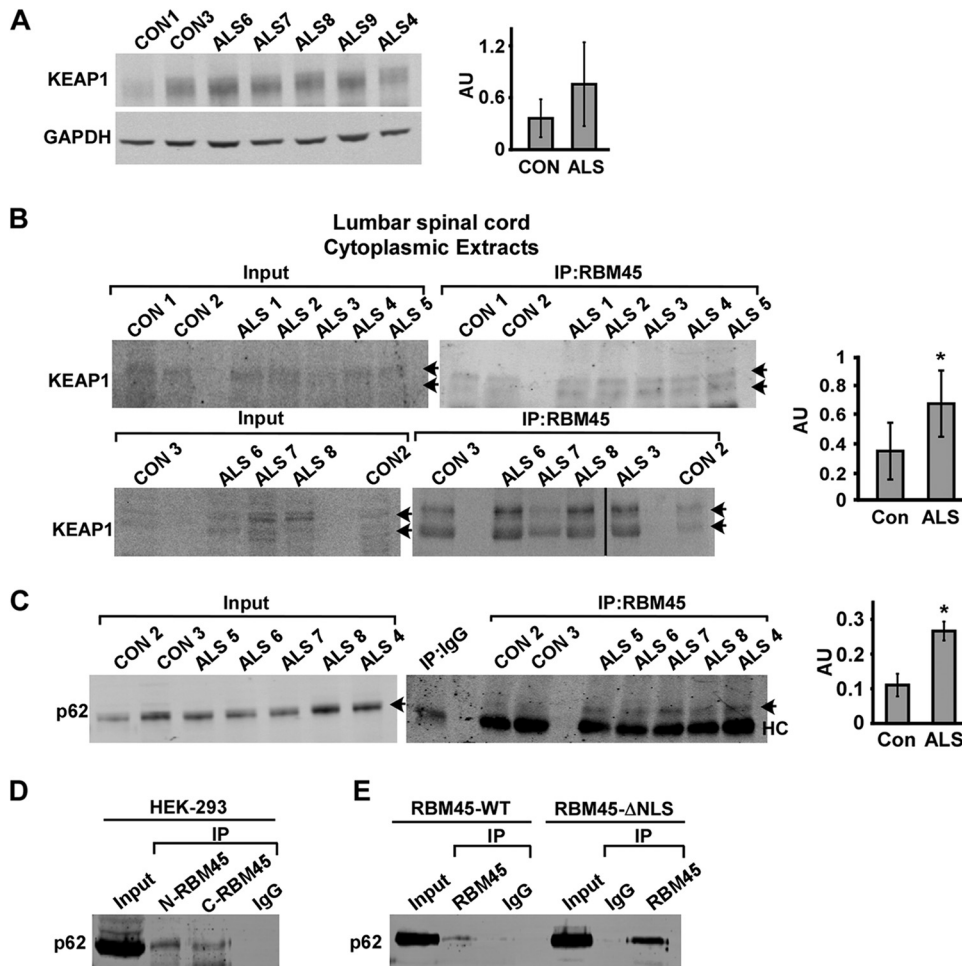
FIG 4 (A) Thirty micrograms of cytoplasmic spinal cord homogenates from ALS cases was run on a gel and probed for KEAP1 and GAPDH. Densitometric analysis of KEAP normalized to GAPDH was performed. (B) Cytoplasmic lumbar spinal cord homogenates (60 μg total protein) were used to immunoprecipitate RBM45. Ten micrograms of each cytoplasmic extract was used for an input control blot (left). The resulting membranes were labeled with antibodies specific to KEAP1. Densitometric analysis was performed to quantify the band intensity normalized to the IgG heavy chain band. Arrows indicate the two KEAP1 isoforms detected. The asterisk denotes a P value of ≤0.05. AU, arbitrary units. (C) Cytoplasmic lumbar spinal cord homogenates were immunoprecipitated as described above for panel A, and membranes were probed for p62 (denoted by an arrow). Forty micrograms of proteins was loaded for the input. HC denotes the IgG heavy chain. Data from densitometric analyses are shown, with a P value of 0.003. (D) Cytoplasmic lysates from HEK-293 cells were prepared and used to immunoprecipitate RBM45 by using two different antibodies (N or C terminus of RBM45) or an isotype IgG control. Eluates along with pre-IP inputs were analyzed by gel electrophoresis and probed for p62. (E) HEK-293 cells overexpressing RBM45-WT or RBM45-ΔNLS were prepared for immunoprecipitation using the antibody to the C terminus of RBM45, as described above for panel D.

similar to those with knockdown of RBM45 (Fig. 5I), further suggesting that increased cell death was indeed mediated by the KEAP1/RBM45 interaction.

Given that RBM45 stabilized KEAP1, we next asked if this stabilization interfered with signal-induced KEAP1 degradation. To this end, we used a potent NRF2 activator, tBHQ, and treated RBM45-overexpressing cells (Fig. 6A). tBHQ activates NRF2 by inducing the degradation of KEAP1 and the subsequent stabilization and activation of NRF2 (48). Indeed, when HEK-293 cells were treated with tBHQ for 16 h, KEAP1 levels decreased, reflecting its degradation (Fig. 6A). RBM45 overexpression increased basal KEAP1 levels, as expected. Interestingly, tBHQ still caused KEAP1 ubiquitination and degradation with kinetics similar to those in vector control-expressing cells, suggesting that RBM45 does not block KEAP1 regulation in response to the potent NRF2 activator tBHQ.

We next sought to examine NRF2 promoter binding activity using reporter assays. Vector-expressing cells treated with tBHQ showed a 2-fold increase in luciferase reporter activity (Fig. 6B). While in RBM45-overexpressing cells, tBHQ treatment induced some NRF2 activity compared to untreated cells (Fig. 6B, black bars), this induction was minimal, suggesting compromised NRF2 activation or at least dampening of NRF2 function.

To explore the consequences of RBM45-induced modulation of NRF2 activation in response to oxidative stress, we treated HEK-293 cells expressing different RBM45 truncations with H_2O_2 and measured ROS production (Fig. 6C). Since RBM45 truncations increased basal levels of ROS production, we calculated fold increases in ROS over untreated cells for each RBM45 construct. While the vector alone showed a 50% increase in ROS levels in response to H_2O_2, wild-type RBM45 overexpression dramatically increased ROS formation, consistent with a compromised antiox-
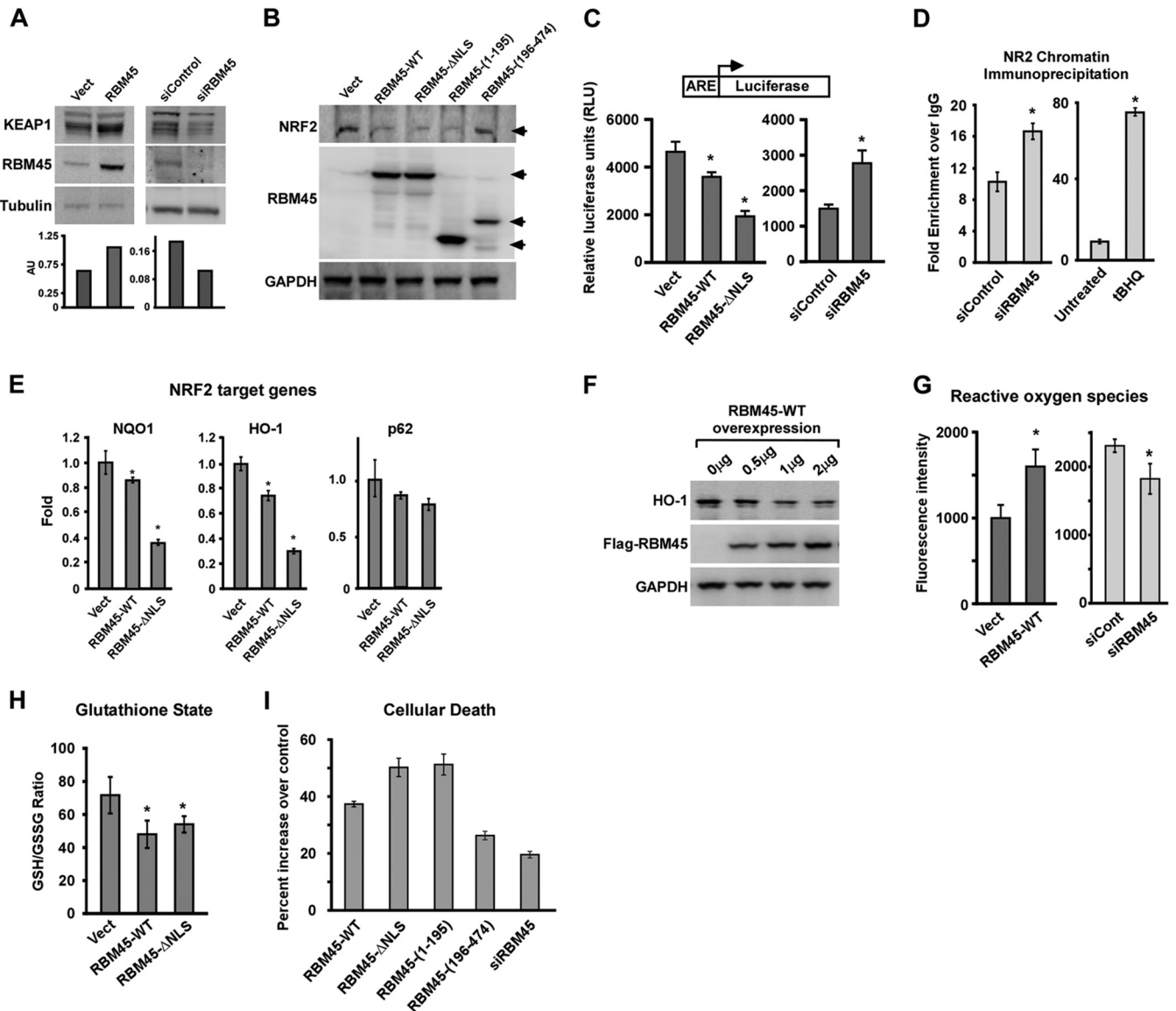
FIG 5 (A) HEK-293 cells were transfected with an empty vector or the RBM45 expression construct (left) or with the indicated siRNA oligonucleotides (right). Cells were harvested 48 h later, and lysates were prepared for Western blot analysis. Membranes were probed for KEAP or RBM45, and β-tubulin was used for loading efficiency. Data from densitometric analysis are shown below the Western blots. (B) HEK-293 cells were transfected with different mutant RBM45 expression constructs and lysed, and Western blotting was performed on protein lysates, probing for NRF2, RBM45, or GAPDH. (C) HEK-293 cells were transfected with the ARE-luciferase reporter construct as well as the indicated expression constructs or siRNA oligonucleotides. Cells were lysed 48 h later, and luciferase activity was measured. Asterisks denotes significant results compared to the vector controls ($P < 0.05$). (D) HEK-293 cells were transfected with control siRNA (siControl) or siRNA against RBM45 (siRBM45) (left) or treated with tBHQ (75 μM for 16 h) prior to formaldehyde cross-linking and immunoprecipitation with an NRF2 antibody or an isotype-specific IgG control. DNA-protein complexes were reverse cross-linked, DNA was isolated, and the ARE on the NQO1 gene was amplified by real-time PCR. C_T (threshold cycle) values were normalized to the corresponding inputs and plotted as fold enrichment over IgG. (E) HEK-293 cells were transfected with the RBM45-WT or RBM45-ΔNLS expression construct, and RNA was extracted. NRF2 target gene expression was determined by real-time RT-PCR. Fold changes normalized to GAPDH values were calculated and averaged across 2 independent experiments. (F) HEK-293 cells were transfected with different amounts of the RBM45-WT expression construct as described above for panel B, and lysates were probed for HO-1. (G) HEK-293 cells overexpressing a vector control or RBM45 or cells transfected with control siRNA or siRNA against RBM45 were incubated with the DCFDA fluorogenic dye for 45 min, followed by PBS washes and fluorescence readout to detect ROS levels. (H) Oxidized and total glutathione contents in HEK-293 cells expressing a vector control, wild-type RBM45, or RBM45-ΔNLS were determined. The ratio of reduced glutathione (GSH) to oxidized glutathione (GSSG) was calculated as an indicator of oxidative stress, with lower ratios indicating increased stress. (I) HEK-293 cells were transfected with various RBM45 deletion constructs or siRNA oligonucleotides, and cell death was determined by using the CellTox green assay (Promega). Results were plotted as the percent increase over vector control-transfected cells (all groups were significantly different from the controls). For all experiments, asterisks denote a statistically significant alteration, as determined from 3 independent experiments ($P < 0.05$).
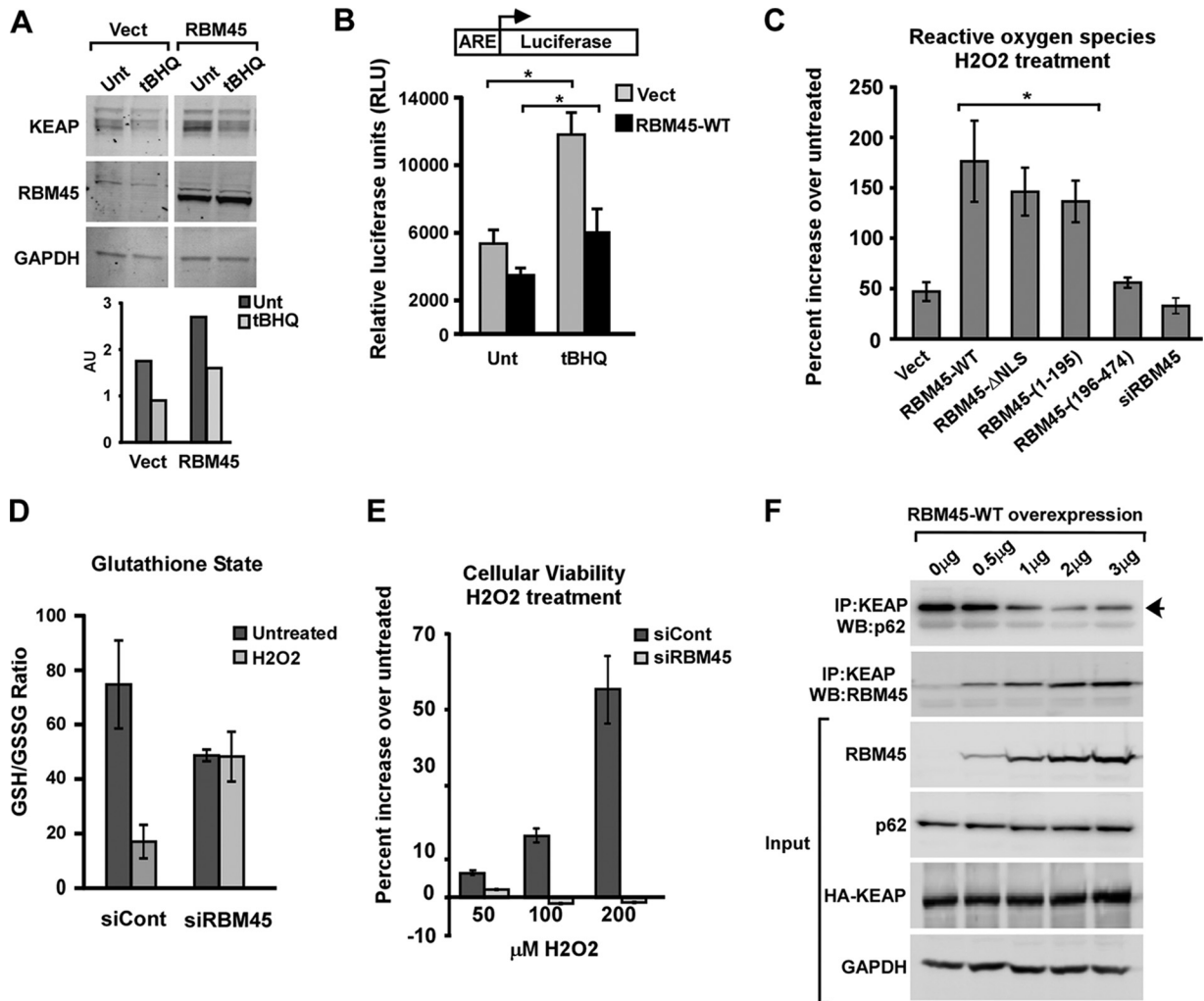
FIG 6 (A) HEK-293 cells stably expressing RBM45 or the vector control were treated with 75 µM tBHQ for 8 h, and cells were harvested for Western blot analysis. Densitometric analysis of KEAP normalized to GAPDH levels was performed, and data were plotted. AU, arbitrary units. (B) Stable cell lines expressing RBM45 or a vector control were transfected with the ARE-luciferase and cytomegalovirus-LacZ reporter constructs. Cells were treated 24 h later with 50 µM tBHQ for 16 h and harvested for luciferase activity measurements. β-Gal assays were performed to assess transfection efficiency. Asterisks denote significant differences from untreated vector-expressing cells ($P < 0.05$). (C) HEK-293 cells were transfected with various RBM45 deletion constructs or siRNA oligonucleotides. Cells were allowed to recover for 24 h and then treated with 50 µM H_2O_2 for 16 h, and cell death was measured by a CellTox green cytotoxicity assay. Results were plotted for each group as the percent increase over the respective untreated cells. The asterisk denotes significant differences from vector controls ($P < 0.05$). Results shown are data from a representative experiment repeated twice. (D) HEK-293 cells were transfected with siRNA oligonucleotides against a control sequence or RBM45 and then treated with 100 µM H_2O_2 for 1 h. Total and oxidized glutathione were then measured and plotted as the ratio of reduced to oxidized glutathione. Results shown are data from a representative experiment repeated three times. (E) HEK-293 cells transfected with siRNA against RBM45 or a scrambled sequence were treated with different doses of H_2O_2 for 4 h, and cellular viability was determined and plotted for each group as the percent change over untreated cells. Results shown are data from a representative experiment repeated twice. (F) HEK-293 cells stably expressing HA-KEAP were transfected with increasing amounts of the RBM45 expression vector. Cells were then lysed, and HA-KEAP was immunoprecipitated to check for binding partners. Pre-IP inputs were run on parallel gels and probed with KEAP, RBM45, p62, and GAPDH.

idant response (Fig. 6C). Similar findings were observed with the cytoplasmic RBM45-ΔNLS and RBM45-(1–195) truncation mutants, suggesting that these effects resulted from increased RBM45 binding to KEAP1. Conversely, cells that express a form of RBM45 that cannot bind KEAP1 [RBM45-(196–474)] or have a knockdown of RBM45 showed ROS levels similar to those of the vector controls, in turn rendering them more resistant to decreased oxidized glutathione (Fig. 6D) and to cell death (Fig. 6E).

Finally, we transfected increasing amounts of RBM45 to determine if increased binding of RBM45 to KEAP1 alters the dynamics of the KEAP1/NRF2 complex. Although we were unable to show differ-ences in NRF2 or Cul3 binding to KEAP1 in the presence of increas-ing amounts of RBM45, we observed decreased binding of KEAP1 to p62 as more RBM45 was recruited to bind KEAP1 (Fig. 6F). Since p62 is a ubiquitin binding protein that targets proteins for degradation, our data suggest that increased RBM45 levels protect KEAP1 from being marked for ubiquitin-mediated degradation, thus stabilizing and increasing the basal levels of this protein.

DISCUSSION

Several independent or interdependent pathogenic mechanisms have been shown to contribute to motor neuron damage in ALS,
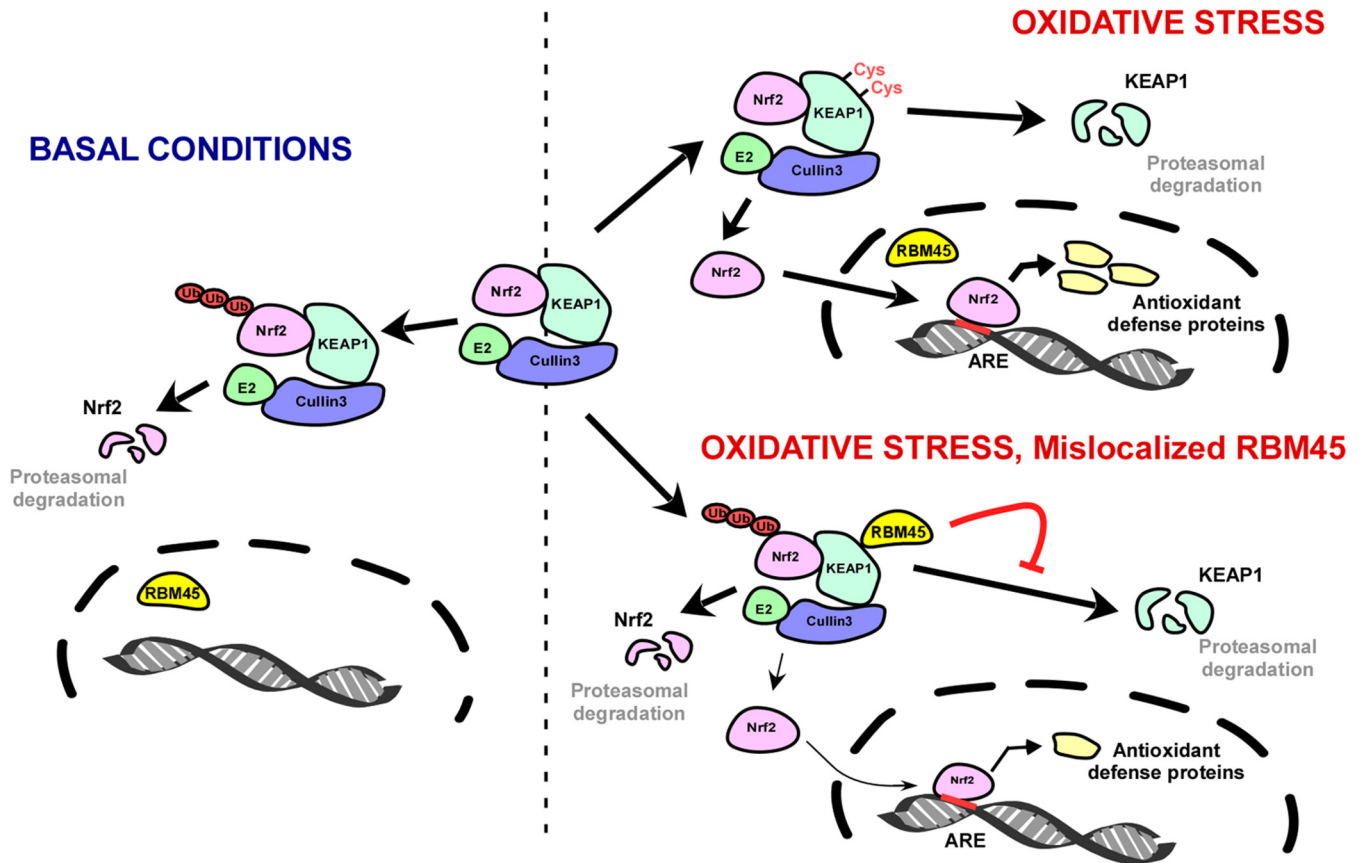
FIG 7 Schematic diagram showing the role of RBM45 in the antioxidant response pathway. Under basal conditions, RBM45 is localized to the nucleus, and KEAP1 is bound to NRF2 in the cytoplasm. KEAP1 recruits the ubiquitin ligase Cul3, which targets NRF2 for ubiquitin-mediated degradation. Oxidative stress signals result in KEAP1 degradation, thus freeing and stabilizing NRF2, which migrates to the nucleus to bind to the ARE on its target genes. NRF2 target genes include those for multiple antioxidant response proteins that mount the cellular antioxidant response. Under yet-to-be-determined conditions, such as chronic oxidative stress or other ALS-specific pathologies, RBM45 nuclear exit (along with cytoplasmic inclusion formation) occurs. Once in the cytoplasm, RBM45 binds KEAP1 and prevents its degradation, thus interfering with NRF2 stabilization. This in turn results in less NRF2 nuclear entry in response to oxidative stress and reduces the cellular antioxidant response, thus contributing to the pathobiology of ALS.

including excitotoxicity, altered axonal transport, mitochondrial dysfunction, protein aggregation, and oxidative stress. Whether oxidative stress is a primary event or merely a consequence of neurodegeneration in ALS is unclear; nevertheless, evidence for increased oxidative stress and ROS generation in both ALS patients and ALS transgenic models suggests that this pathway is a major contributory factor in motor neuron death (49, 50). KEAP1 has been shown to localize to neuronal and cytoplasmic p62-positive inclusions in neurodegenerative diseases, including ALS (32), and altered levels of both NRF2 and KEAP1 as well as their downstream targets in ALS have also been described (27, 31). In our current study, we demonstrate that a nuclear RNA binding protein, RBM45, can be translocated into the cytoplasm and modulate the KEAP1/NRF2 antioxidant response pathway (Fig. 7). Our results demonstrate that RBM45 can localize to cytoplasmic stress granules in response to oxidative stress, and this redistribution increases its binding to the KEAP1 antioxidant response inhibitor. We validated this binding of RBM45 to KEAP1 in ALS lumbar spinal cord and further revealed the physiological consequence of such increased binding, namely, increased stability of the antioxidant response inhibitor. Increased KEAP1 protein levels due to cytoplasmic RBM45 inhibit NRF2 activity and reduce the cellular

antioxidant response, thus keeping ROS levels elevated and contributing to cellular death (Fig. 7). Our findings therefore support a novel role for an ALS-associated RNA binding protein, RBM45, in the direct regulation of the antioxidant response in ALS. In addition, we propose a new mechanism by which RNA binding proteins can contribute to motor neuron death beyond protein aggregation or altered RNA metabolism.

Human *NRF2* has been shown to be highly polymorphic, with a mutagenic frequency of 1 per 72 bp (51, 52). Variations in its promoter have been shown to affect NRF2 protein expression and to be associated with various diseases, including neurodegenerative diseases such as Parkinson's disease and Alzheimer's disease (53, 54). Given the central role of NRF2 and KEAP1 in the antioxidant pathway, and the multitude of evidence for oxidative stress in ALS, it is no surprise that multiple laboratories have investigated the association between *NRF2* and *KEAP1* haplotypes and ALS. LoGerfo et al. asked whether polymorphisms in the *NRF2* promoter could functionally affect the protein's function, thereby altering oxidative stress markers in ALS, but found no correlations between these two variables (52). Bergstrom and colleagues analyzed multiple single nucleotide polymorphisms (SNPs) in *NRF2* and *KEAP1* in a Swedish cohort to look for dif-

ferences in risk for ALS, age at onset, and survival (55). No SNP was associated with risk or survival, but the authors identified one haplotype in the *NRF2* promoter characterized by higher NRF2 protein expression levels that was associated with disease onset 4 years later and one in *KEAP1* that was associated with a later onset of ALS. Given the lack of mutations in the KEAP1/NRF2 complex and the fact that oxidative stress is common in ALS, one may speculate that other regulators of this pathway may contribute to modulating oxidative stress in ALS. Indeed, multiple mutations in p62/sqstm1 have been described in ALS (44), and we propose that the altered subcellular distribution of RBM45 in ALS is yet another factor contributing to the dysfunctional antioxidant response.

Antioxidant-based therapies for ALS have so far not shown efficacy in clinical trials (56, 57). In addition, knockout or overexpression of NRF2 in neurons and muscle in mutant SOD1 animal models has shown a modest impact on the course of disease (28, 29). Intramuscular adeno-associated virus 6 (AAV6)-mediated delivery of the antioxidant gene *PRDX3* or *NRF2* likewise failed to affect survival, disease onset, or progression in a similar mutant SOD1 ALS model (58). While the overexpression of mutant SOD1 in these model systems may negatively impact the ability of antioxidant-based treatments to alter the disease course, another possibility is that other modulators of the oxidant response pathway may play key roles in impeding antioxidant responses in these ALS model systems and thus contribute to neuronal cell death. We observed RBM45 cytoplasmic inclusions in motor neurons of ALS and frontotemporal lobar degeneration (FTLD) patients, and in this study, we demonstrate that RBM45 binds and stabilizes KEAP1 when located in the cytoplasm, having a deleterious effect on cellular survival. Impeding the KEAP1/NRF2 oxidant response pathway is a novel function for RBM45, suggesting that more direct activators of NRF2 activity may be required to restore antioxidant responses in neurodegenerative diseases. A recent comprehensive *in vitro* screening of NRF2 activators identified $S[+]$-apomorphine as a promising target with CNS penetrance (59). The authors of that study validated the neuroprotective potential of this compound in the mutant SOD1 ALS mouse model and, more importantly, in fibroblasts derived from both sporadic and familial ALS patients who harbor SOD1 mutations.

Although RBM45 has a structure similar to those of other inclusion-forming ALS-linked RNA binding proteins such as TDP-43 and FUS, and although RBM45 has been shown to interact with TDP-43 (11), we believe that the proposed role of RBM45 in modulating the oxidative stress response is novel among RNA binding proteins. A previously reported proteomic analysis of KEAP1-interacting proteins did not detect TDP-43, FUS, or other RNA binding proteins (47). We were similarly unable to show direct binding between KEAP1 and either FUS or TDP-43 (data not shown). Therefore, we conclude that the cytoplasmic role of RBM45 in binding KEAP1 and inhibiting the antioxidant response is a unique feature of this particular RNA binding protein.

Nevertheless, while TDP-43 and FUS fail to interact with KEAP1, there are commonalities between RBM45, FUS, and TDP-43 in response to oxidative stress. TDP-43 has been shown to accumulate in cytoplasmic stress granules under conditions of oxidative stress, including arsenite and Paraquat treatment of cultured cells, a phenotype that requires its first RRM and is regulated by c-Jun N-terminal kinase (c-JNK) (60–62). Similarly, we demonstrate that RBM45 exits the nucleus and localizes to cytoplasmic TIAR-positive stress granules in response to oxidative stress. In-

terestingly, we observed this RBM45 stress response in primary motor neurons and differentiated SH-SY5Y cells but not in undifferentiated NSC-34 cells, a motor neuron-like cell line. It is possible that the RBM45 response to stress is cell type specific or occurs only in differentiated neurons and thus may contribute to the selective neurodegeneration that occurs in ALS and other neurodegenerative diseases. Further studies are required to explore this hypothesis. In addition, we find that overexpression of RBM45-ΔNLS results in cytoplasmic granule formation, reminiscent of the phenotype observed for ALS spinal cord and hippocampus (data not shown). We demonstrate that the first two RRM domains of RBM45 are required for binding to KEAP1 and mediate increased cellular toxicity in response to oxidative insults, although their exact role in stress granule accumulation remains unknown. The accumulation of TDP-43 and other RNA binding proteins in cytoplasmic stress granules may be a more generalized response to eliminate aggregated or mislocalized proteins, whereas RBM45 effectively binds and stabilizes KEAP1 when located at the cytoplasm or stress granules. In addition, RBM45 was recently identified as a TDP-43 binding partner by using a yeast two-hybrid system that used the C-terminal fragment of TDP-43 implicated in ALS (11), suggesting that the two proteins could be functioning as part of similar pathways in disease. More importantly, both RBM45 and TDP-43 have been shown to partially colocalize to cytoplasmic inclusions in motor neurons of ALS spinal cords (9, 63). It is unclear whether RBM45 and TDP-43 exit the nucleus independently or via the same mechanism in ALS and under oxidative stress conditions. In summary, we have described a novel role for RBM45 in regulating the antioxidant response inhibitor KEAP1 through a direct protein-protein interaction, thus inhibiting the neuroprotective antioxidant response.

ACKNOWLEDGMENTS

REFERENCES

1. **Kiernan MC, Vucic S, Cheah BC, Turner MR, Eisen A, Hardiman O, Burrell JR, Zoing MC.** 2011. Amyotrophic lateral sclerosis. Lancet **377:** 942–955. http://dx.doi.org/10.1016/S0140-6736(10)61156-7.

2. **Pratt AJ, Getzoff ED, Perry JJ.** 2012. Amyotrophic lateral sclerosis: update and new developments. Degener Neurol Neuromuscul Dis **2012:** 1–14. http://dx.doi.org/10.2147/DNND.S19803.

3. **Byrne S, Walsh C, Lynch C, Bede P, Elamin M, Kenna K, McLaughlin R, Hardiman O.** 2011. Rate of familial amyotrophic lateral sclerosis: a systematic review and meta-analysis. J Neurol Neurosurg Psychiatry **82:** 623–627. http://dx.doi.org/10.1136/jnnp.2010.224501.

4. **Leigh PN, Whitwell H, Garofalo O, Buller J, Swash M, Martin JE, Gallo J-M, Weller RO, Anderton BH.** 1991. Ubiquitin-immunoreactive intraneuronal inclusions in amyotrophic lateral sclerosis; morphology, distribution and specificity. Brain **114:** 775–788. http://dx.doi.org/10.1093/brain/114.2.775.

5. **Turner MR, Bowser R, Bruijn L, Dupuis L, Ludolph A, McGrath M,**

Manfredi G, Maragakis N, Miller RG, Pullman SL, Rutkove SB, Shaw PJ, Shefner J, Fischbeck KH. 2013. Mechanisms, models and biomarkers in amyotrophic lateral sclerosis. Amyotroph Lateral Scler Frontotemporal Degener **14**(Suppl 1):19–32. http://dx.doi.org/10.3109/21678421.2013.778554.

6. Lagier-Tourenne C, Polymenidou M, Cleveland DW. 2010. TDP-43 and FUS/TLS: emerging roles in RNA processing and neurodegeneration. Hum Mol Genet **19**:R46–R64. http://dx.doi.org/10.1093/hmg/ddq137.

7. Verma A, Tandan R. 2013. RNA quality control and protein aggregates in amyotrophic lateral sclerosis: a review. Muscle Nerve **47**:330–338. http://dx.doi.org/10.1002/mus.23673.

8. Li YR, King OD, Shorter J, Gitler AD. 2013. Stress granules as crucibles of ALS pathogenesis. J Cell Biol **201**:361–372. http://dx.doi.org/10.1083/jcb.201302044.

9. Collins M, Riascos D, Kovalik T, An J, Krupa K, Hood BL, Conrads TP, Renton AE, Traynor BJ, Bowser R. 2012. The RNA-binding motif 45 (RBM45) protein accumulates in inclusion bodies in amyotrophic lateral sclerosis (ALS) and frontotemporal lobar degeneration with TDP-43 inclusions (FTLD-TDP) patients. Acta Neuropathol **124**:717–732. http://dx.doi.org/10.1007/s00401-012-1045-x.

10. Tamada H, Sakashita E, Shimazaki K, Ueno E, Hamamoto T, Kagawa Y, Endo H. 2002. cDNA cloning and characterization of Drb1, a new member of RRM-type neural RNA-binding protein. Biochem Biophys Res Commun **297**:96–104. http://dx.doi.org/10.1016/S0006-291X(02)02132-0.

11. Hans F, Fiesel FC, Strong JC, Jackel S, Rasse TM, Geisler S, Springer W, Schulz JB, Voigt A, Kahle PJ. 2014. UBE2E ubiquitin-conjugating enzymes and ubiquitin isopeptidase Y regulate TDP-43 protein ubiquitination. J Biol Chem **289**:19164–19179. http://dx.doi.org/10.1074/jbc.M114.561704.

12. Halliwell B. 2006. Oxidative stress and neurodegeneration: where are we now? J Neurochem **97**:1634–1658. http://dx.doi.org/10.1111/j.1471-4159.2006.03907.x.

13. Aguirre N, Beal MF, Matson WR, Bogdanov MB. 2005. Increased oxidative damage to DNA in an animal model of amyotrophic lateral sclerosis. Free Radic Res **39**:383–388. http://dx.doi.org/10.1080/10715760400027979.

14. Andrus PK, Fleck TJ, Gurney ME, Hall ED. 1998. Protein oxidative damage in a transgenic mouse model of familial amyotrophic lateral sclerosis. J Neurochem **71**:2041–2048.

15. Ferrante RJ, Shinobu LA, Schulz JB, Matthews RT, Thomas CE, Kowall NW, Gurney ME, Beal MF. 1997. Increased 3-nitrotyrosine and oxidative damage in mice with a human copper/zinc superoxide dismutase mutation. Ann Neurol **42**:326–334. http://dx.doi.org/10.1002/ana.410420309.

16. Miana-Mena FJ, Gonzalez-Mingot C, Larrode P, Munoz MJ, Olivan S, Fuentes-Broto L, Martinez-Ballarin E, Reiter RJ, Osta R, Garcia JJ. 2011. Monitoring systemic oxidative stress in an animal model of amyotrophic lateral sclerosis. J Neurol **258**:762–769. http://dx.doi.org/10.1007/s00415-010-5825-8.

17. Nikolic-Kokic A, Stevic Z, Blagojevic D, Davidovic B, Jones DR, Spasic MB. 2006. Alterations in anti-oxidative defence enzymes in erythrocytes from sporadic amyotrophic lateral sclerosis (SALS) and familial ALS patients. Clin Chem Lab Med **44**:589–593. http://dx.doi.org/10.1515/CCLM.2006.111.

18. Simpson EP, Henry YK, Henkel JS, Smith RG, Appel SH. 2004. Increased lipid peroxidation in sera of ALS patients: a potential biomarker of disease burden. Neurology **62**:1758–1765. http://dx.doi.org/10.1212/WNL.62.10.1758.

19. Ferrante RJ, Browne SE, Shinobu LA, Bowling AC, Baik MJ, MacGarvey U, Kowall NW, Brown RH, Jr, Beal MF. 1997. Evidence of increased oxidative damage in both sporadic and familial amyotrophic lateral sclerosis. J Neurochem **69**:2064–2074.

20. D'Amico E, Factor-Litvak P, Santella RM, Mitsumoto H. 2013. Clinical perspective of oxidative stress in sporadic ALS. Free Radic Biol Med **65**:509–527. http://dx.doi.org/10.1016/j.freeradbiomed.2013.06.029.

21. Zhang DD. 2006. Mechanistic studies of the Nrf2-Keap1 signaling pathway. Drug Metab Rev **38**:769–789. http://dx.doi.org/10.1080/03602530600971974.

22. Taguchi K, Motohashi H, Yamamoto M. 2011. Molecular mechanisms of the Keap1-Nrf2 pathway in stress response and cancer evolution. Genes Cells **16**:123–140. http://dx.doi.org/10.1111/j.1365-2443.2010.01473.x.

23. Tong KI, Kobayashi A, Katsuoka F, Yamamoto M. 2006. Two-site substrate recognition model for the Keap1-Nrf2 system: a hinge and latch mechanism. Biol Chem **387**:1311–1320. http://dx.doi.org/10.1515/BC.2006.164.

24. Komatsu M, Kurokawa H, Waguri S, Taguchi K, Kobayashi A, Ichimura Y, Sou YS, Ueno I, Sakamoto A, Tong KI, Kim M, Nishito Y, Iemura S, Natsume T, Ueno T, Kominami E, Motohashi H, Tanaka K, Yamamoto M. 2010. The selective autophagy substrate p62 activates the stress responsive transcription factor Nrf2 through inactivation of Keap1. Nat Cell Biol **12**:213–223. http://dx.doi.org/10.1038/ncb2021.

25. Chorley BN, Campbell MR, Wang X, Karaca M, Sambandan D, Bangura F, Xue P, Pi J, Kleeberger SR, Bell DA. 2012. Identification of novel NRF2-regulated genes by ChIP-Seq: influence on retinoid X receptor alpha. Nucleic Acids Res **40**:7416–7429. http://dx.doi.org/10.1093/nar/gks409.

26. Mimoto T, Miyazaki K, Morimoto N, Kurata T, Satoh K, Ikeda Y, Abe K. 2012. Impaired antioxydative Keap1/Nrf2 system and the downstream stress protein responses in the motor neuron of ALS model mice. Brain Res **1446**:109–118. http://dx.doi.org/10.1016/j.brainres.2011.12.064.

27. Kraft AD, Resch JM, Johnson DA, Johnson JA. 2007. Activation of the Nrf2-ARE pathway in muscle and spinal cord during ALS-like pathology in mice expressing mutant SOD1. Exp Neurol **207**:107–117. http://dx.doi.org/10.1016/j.expneurol.2007.05.026.

28. Guo Y, Zhang Y, Wen D, Duan W, An T, Shi P, Wang J, Li Z, Chen X, Li C. 2013. The modest impact of transcription factor Nrf2 on the course of disease in an ALS animal model. Lab Invest **93**:825–833. http://dx.doi.org/10.1038/labinvest.2013.73.

29. Vargas MR, Burton NC, Kutzke J, Gan L, Johnson DA, Schafer M, Werner S, Johnson JA. 2013. Absence of Nrf2 or its selective overexpression in neurons and muscle does not affect survival in ALS-linked mutant hSOD1 mouse models. PLoS One **8**:e56625. http://dx.doi.org/10.1371/journal.pone.0056625.

30. Vargas MR, Johnson DA, Sirkis DW, Messing A, Johnson JA. 2008. Nrf2 activation in astrocytes protects against neurodegeneration in mouse models of familial amyotrophic lateral sclerosis. J Neurosci **28**:13574–13581. http://dx.doi.org/10.1523/JNEUROSCI.4099-08.2008.

31. Sarlette A, Krampfl K, Grothe C, Neuhoff N, Dengler R, Petri S. 2008. Nuclear erythroid 2-related factor 2-antioxidative response element signaling pathway in motor cortex and spinal cord in amyotrophic lateral sclerosis. J Neuropathol Exp Neurol **67**:1055–1062. http://dx.doi.org/10.1097/NEN.0b013e31818b4906.

32. Tanji K, Maruyama J, Odagiri S, Mori F, Itoh K, Kakita A, Takahashi H, Wakabayashi K. 2013. Keap1 is localized in neuronal and glial cytoplasmic inclusions in various neurodegenerative diseases. J Neuropathol Exp Neurol **72**:18–28. http://dx.doi.org/10.1097/NEN.0b013e31827b5713.

33. Guo Y, Wang Q, Zhang K, An T, Shi P, Li Z, Duan W, Li C. 2012. HO-1 induction in motor cortex and intestinal dysfunction in TDP-43 A315T transgenic mice. Brain Res **1460**:88–95. http://dx.doi.org/10.1016/j.brainres.2012.04.003.

34. Duan W, Li X, Shi J, Guo Y, Li Z, Li C. 2010. Mutant TAR DNA-binding protein-43 induces oxidative injury in motor neuron-like cell. Neuroscience **169**:1621–1629. http://dx.doi.org/10.1016/j.neuroscience.2010.06.018.

35. Furukawa M, Xiong Y. 2005. BTB protein Keap1 targets antioxidant transcription factor Nrf2 for ubiquitination by the Cullin 3-Roc1 ligase. Mol Cell Biol **25**:162–171. http://dx.doi.org/10.1128/MCB.25.1.162-171.2005.

36. Kolarcik C, Bowser R. 2012. Retinoid signaling alterations in amyotrophic lateral sclerosis. Am J Neurodegener Dis **1**:130–145.

37. Graber DJ, Harris BT. 2013. Purification and culture of spinal motor neurons from rat embryos. Cold Spring Harb Protoc **2013**:319–326. http://dx.doi.org/10.1101/pdb.prot074161.

38. Ponti A, Schwarb P, Gulati A, Bäcker V. 2007. Huygens Remote Manager, a Web interface for high-volume batch deconvolution. Imaging Microsc **9**:57–58. http://dx.doi.org/10.1002/imic.200790154.

39. Parker SJ, Meyerowitz J, James JL, Liddell JR, Crouch PJ, Kanninen KM, White AR. 2012. Endogenous TDP-43 localized to stress granules can subsequently form protein aggregates. Neurochem Int **60**:415–424. http://dx.doi.org/10.1016/j.neuint.2012.01.019.

40. Mazan-Mamczarz K, Lal A, Martindale JL, Kawai T, Gorospe M. 2006. Translational repression by RNA-binding protein TIAR. Mol Cell Biol **26**:2716–2727. http://dx.doi.org/10.1128/MCB.26.7.2716-2727.2006.

41. Taupin JL, Tian Q, Kedersha N, Robertson M, Anderson P. 1995. The RNA-binding protein TIAR is translocated from the nucleus to the cytoplasm during Fas-mediated apoptotic cell death. Proc Natl Acad Sci U S A **92**:1629–1633. http://dx.doi.org/10.1073/pnas.92.5.1629.

42. **Seibenhener ML, Babu JR, Geetha T, Wong HC, Krishna NR, Wooten MW.** 2004. Sequestosome 1/p62 is a polyubiquitin chain binding protein involved in ubiquitin proteasome degradation. Mol Cell Biol **24**:8055–8068. http://dx.doi.org/10.1128/MCB.24.18.8055-8068.2004.

43. **Fecto F, Yan J, Vemula SP, Liu E, Yang Y, Chen W, Zheng JG, Shi Y, Siddique N, Arrat H, Donkervoort S, Ajroud-Driss S, Sufit RL, Heller SL, Deng HX, Siddique T.** 2011. SQSTM1 mutations in familial and sporadic amyotrophic lateral sclerosis. Arch Neurol **68**:1440–1446. http://dx.doi.org/10.1001/archneurol.2011.250.

44. **Teyssou E, Takeda T, Lebon V, Boillee S, Doukoure B, Bataillon G, Sazdovitch V, Cazeneuve C, Meininger V, LeGuern E, Salachas F, Seilhean D, Millecamps S.** 2013. Mutations in SQSTM1 encoding p62 in amyotrophic lateral sclerosis: genetics and neuropathology. Acta Neuropathol **125**:511–522. http://dx.doi.org/10.1007/s00401-013-1090-0.

45. **Gal J, Strom AL, Kilty R, Zhang F, Zhu H.** 2007. p62 accumulates and enhances aggregate formation in model systems of familial amyotrophic lateral sclerosis. J Biol Chem **282**:11068–11077. http://dx.doi.org/10.1074/jbc.M608787200.

46. **Mizuno Y, Amari M, Takatama M, Aizawa H, Mihara B, Okamoto K.** 2006. Immunoreactivities of p62, an ubiquitin-binding protein, in the spinal anterior horn cells of patients with amyotrophic lateral sclerosis. J Neurol Sci **249**:13–18. http://dx.doi.org/10.1016/j.jns.2006.05.060.

47. **Sowa ME, Bennett EJ, Gygi SP, Harper JW.** 2009. Defining the human deubiquitinating enzyme interaction landscape. Cell **138**:389–403. http://dx.doi.org/10.1016/j.cell.2009.04.042.

48. **Zhang DD, Lo SC, Sun Z, Habib GM, Lieberman MW, Hannink M.** 2005. Ubiquitination of Keap1, a BTB-Kelch substrate adaptor protein for Cul3, targets Keap1 for degradation by a proteasome-independent pathway. J Biol Chem **280**:30091–30099. http://dx.doi.org/10.1074/jbc.M501279200.

49. **Barber SC, Shaw PJ.** 2010. Oxidative stress in ALS: key role in motor neuron injury and therapeutic target. Free Radic Biol Med **48**:629–641. http://dx.doi.org/10.1016/j.freeradbiomed.2009.11.018.

50. **Parakh S, Spencer DM, Halloran MA, Soo KY, Atkin JD.** 2013. Redox regulation in amyotrophic lateral sclerosis. Oxid Med Cell Longev **2013**:408681. http://dx.doi.org/10.1155/2013/408681.

51. **Cho HY.** 2013. Genomic structure and variation of nuclear factor (erythroid-derived 2)-like 2. Oxid Med Cell Longev **2013**:286524. http://dx.doi.org/10.1155/2013/286524.

52. **LoGerfo A, Chico L, Borgia L, Petrozzi L, Rocchi A, D'Amelio A, Carlesi C, Caldarazzo Ienco E, Mancuso M, Siciliano G.** 2014. Lack of association between nuclear factor erythroid-derived 2-like 2 promoter gene polymorphisms and oxidative stress biomarkers in amyotrophic lateral sclerosis patients. Oxid Med Cell Longev **2014**:432626. http://dx.doi.org/10.1155/2014/432626.

53. **von Otter M, Landgren S, Nilsson S, Celojevic D, Bergstrom P, Hakansson A, Nissbrandt H, Drozdzik M, Bialecka M, Kurzawski M, Blennow K, Nilsson M, Hammarsten O, Zetterberg H.** 2010. Association of Nrf2-encoding NFE2L2 haplotypes with Parkinson's disease. BMC Med Genet **11**:36. http://dx.doi.org/10.1186/1471-2350-11-36.

54. **von Otter M, Landgren S, Nilsson S, Zetterberg M, Celojevic D, Bergstrom P, Minthon L, Bogdanovic N, Andreasen N, Gustafson DR, Skoog I, Wallin A, Tasa G, Blennow K, Nilsson M, Hammarsten O, Zetterberg H.** 2010. Nrf2-encoding NFE2L2 haplotypes influence disease progression but not risk in Alzheimer's disease and age-related cataract. Mech Ageing Dev **131**:105–110. http://dx.doi.org/10.1016/j.mad.2009.12.007.

55. **Bergstrom P, von Otter M, Nilsson S, Nilsson AC, Nilsson M, Andersen PM, Hammarsten O, Zetterberg H.** 2013. Association of NFE2L2 and KEAP1 haplotypes with amyotrophic lateral sclerosis. Amyotroph Lateral Scler Frontotemporal Degener **15**:130–137. http://dx.doi.org/10.3109/21678421.2013.839708.

56. **Barber SC, Mead RJ, Shaw PJ.** 2006. Oxidative stress in ALS: a mechanism of neurodegeneration and a therapeutic target. Biochim Biophys Acta **1762**:1051–1067. http://dx.doi.org/10.1016/j.bbadis.2006.03.008.

57. **Orrell RW, Lane RJ, Ross M.** 2007. Antioxidant treatment for amyotrophic lateral sclerosis/motor neuron disease. Cochrane Database Syst Rev **2007**:CD002829. http://dx.doi.org/10.1002/14651858.CD002829.pub4.

58. **Nanou A, Higginbottom A, Valori CF, Wyles M, Ning K, Shaw P, Azzouz M.** 2013. Viral delivery of antioxidant genes as a therapeutic strategy in experimental models of amyotrophic lateral sclerosis. Mol Ther **21**:1486–1496. http://dx.doi.org/10.1038/mt.2013.115.

59. **Mead RJ, Higginbottom A, Allen SP, Kirby J, Bennett E, Barber SC, Heath PR, Coluccia A, Patel N, Gardner I, Brancale A, Grierson AJ, Shaw PJ.** 2013. S[+] Apomorphine is a CNS penetrating activator of the Nrf2-ARE pathway with activity in mouse and patient fibroblast models of amyotrophic lateral sclerosis. Free Radic Biol Med **61**:438–452. http://dx.doi.org/10.1016/j.freeradbiomed.2013.04.018.

60. **Colombrita C, Zennaro E, Fallini C, Weber M, Sommacal A, Buratti E, Silani V, Ratti A.** 2009. TDP-43 is recruited to stress granules in conditions of oxidative insult. J Neurochem **111**:1051–1061. http://dx.doi.org/10.1111/j.1471-4159.2009.06383.x.

61. **Meyerowitz J, Parker SJ, Vella LJ, Ng D, Price KA, Liddell JR, Caragounis A, Li QX, Masters CL, Nonaka T, Hasegawa M, Bogoyevitch MA, Kanninen KM, Crouch PJ, White AR.** 2011. C-Jun N-terminal kinase controls TDP-43 accumulation in stress granules induced by oxidative stress. Mol Neurodegener **6**:57. http://dx.doi.org/10.1186/1750-1326-6-57.

62. **Yamaguchi A, Kitajo K.** 2012. The effect of PRMT1-mediated arginine methylation on the subcellular localization, stress granules, and detergent-insoluble aggregates of FUS/TLS. PLoS One **7**:e49267. http://dx.doi.org/10.1371/journal.pone.0049267.

63. **Neumann M, Sampathu DM, Kwong LK, Truax AC, Miscenyi MC, Chou LT, Bruce J, Schuck T, Grossman M, Clark CM, McCluskey LF, Miller BL, Masliah E, Mackenzie IR, Feldman H, Feiden W, Kretzschmar HA, Trojanowski JQ, Lee VM.** 2006. Ubiquitinated TDP-43 in frontotemporal lobar degeneration and amyotrophic lateral sclerosis. Science **314**:130–133. http://dx.doi.org/10.1126/science.1134108.